Journal of New Technology and Materials (JNTM)
J. New Technol. Mater.
Vol. 08, N°02 (2018)33-37

OEB Univ. Publish. Co.

Electrodeposition and characterization of ZnS nanostructures for solar cells application

K. Ghezali[a, b], L. Mentar[b,*], B. Boudine[a] and A. Azizi[b]

[a]*Laboratoire de Cristallographie, Département de Physique, Faculté des Sciences Exactes Université Mentouri - Constantine 1*
[b]*Laboratoire de Chimie, Ingénierie Moléculaires et Nanostructures, Université Sétif1, Algérie*
menter.loubna@yahoo.com

Received date: Jul. 07, 2017; revised date: Jul. 4, 2018; accepted date: Sep. 18, 2018

Abstract

In the last few years, metal oxides nanostructures have attracted quickly increasing attention, due to their very interesting properties .Among them, Zinc sulfide (ZnS) semiconductor is an appropriate candidate as window or buffer layer in solar cells applications. ZnS thin films were prepared at room temperature by electrochemical deposition using zinc sulfate and sodium thiosulfate solution at pH 2.7. In this paper, we investigated the influence of the concentration of zinc sulfate on structural, morphological and optical properties for ZnS thin films electrodeposits.SEM images demonstrated that the morphology of ZnS thin films depend greatly on the intial concentration of $ZnSO_4$. XRD studies confirmed the presence of zinc blende structure. The optical measurements (UV-Vis) show a large band gap between 3.4 –3.9 eV depending on the concentration of zinc sulfate.

Keywords: thin films, ZnS, band gap, carrier density, nanostructures.

1. Introduction

Photovoltaic is the direct conversion of light into electricity at the atomic level using semiconductor materials that exhibit the photovoltaic effect [1]. Semiconductors have widely been used in solar cells application such us Zinc sulfide .ZnS is used in junction with SnS[2], CuO[3] and CZTS[4], it is a potential candidate to replace CdS in junction with CdTe and CIGS [5], as buffer layer or as window layer in multilayers ZnS/CdS/CdTe solar cells [5]. ZnS present many interesting properties, essentially: high transparency, large band gap, n-type conductivity and high exciton binding energy (55meV) [3]. ZnS is a nontoxic, II–VI semiconductor, with a large direct band gap of about 3.7eV. It has a refractive index (n) of 2.40 [6] which also make it suitable for application as antireflective coatings in thin-film solar cells.

Different methods are used to elaborate ZnS thin films such as: Sol gel, spray pyrolysis, chemical vapor deposition, chemical bath deposition, pulsed laser and electrodeposition [7]. The electrodeposition of thin films is considered as one of the promising ways to elaborate materials at a nanometric scale, due to its possibility of controlling thickness, processing for large-area production, low cost fabrication process and low processing temperature. There have been many work on the electrodeposition of ZnS, Effect of sulfosalicylic acid (C7H6O6S) on the electrodeposition of pure ZnS nanocrystal thin films from acidic solutions on electrodeposition was done using the thiosulfate and zinc sulfate or zinc chloride as precursor for the electrodeposition of ZnS [8,5].

In the present work, we report the electrochemical synthesis of ZnS nanostructures on Indium tin oxide (ITO) conducting glass in acidic medium. Two different bath concentrations have been used. The electrochemical, structural, morphological and optical properties of ZnS nanostructures were investigated.

2. Experimental

ZnS films was carried out in a glass three-electrode cell equipped with a saturated calomel electrode (SCE) placed as a reference electrode, platinum plate as a counter electrode and Indium tin oxide (ITO) coated glass substrates as the working electrode. The ITO substrates were ultrasonically cleaned with acetone, methanol and distillate water for 10 min, respectively and then dried in the air. ZnS thin films were electrodeposited potentiostatically from solution contained 10^{-4}M of $Na_2S_2O_3$, 10^{-3} and 10^{-4} M of $ZnSO_4$. The pH was adjustedto 2.7 using diluted H_2SO_4. Films were deposited at potentialof -1.2 vs.SCE using Potentiostat/Galvanostat (PGZ301, Radiometer Analytical). After deposition, the films were rinsed with distillate water and dried in air.

The surface morphology and microstructure of the ZnSnanostrutures were examined using scanning electron microscopy (SEM) JEOL 7800F. Phases identification and crystallographic structure determination were carried out

using XRD Bruker AXS D8 Discover with CuKa1 radiation (k = 1.5418 A °) in a θ - 2θ geometry. The optical properties were observed by UV-Visible spectroscopy JASCO V-670 UV-Vis.

3. Results

3.1 Cyclic voltametry:

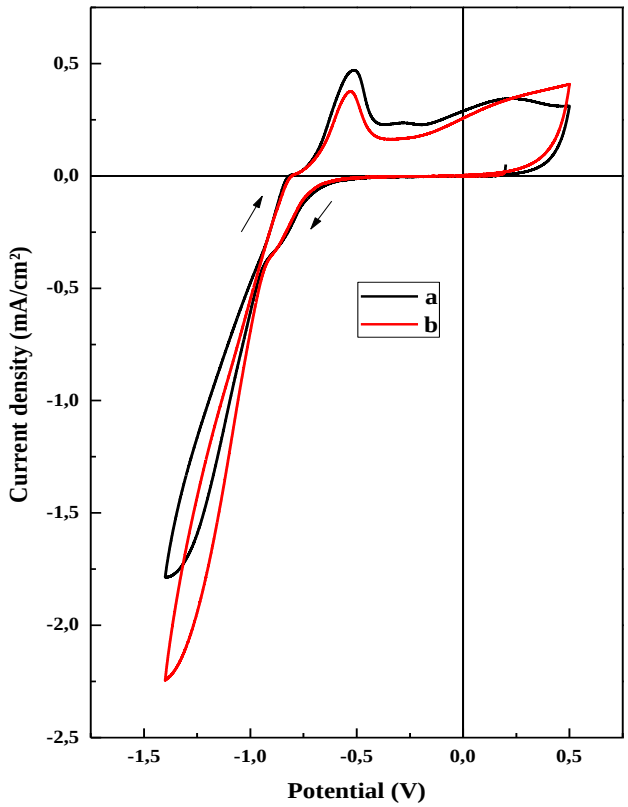

Figure 1. Cyclic Voltammetry for the aqueous solutions containing 10^{-3} M $Na_2S_2O_3$ and a) 10^{-3} M, b) 10^{-4}M of $ZnSO_4$

The voltammograms in Fig. 01 shown the behavior of the ITO substrate in a solution containing 10^{-3} M $Na_2S_2O_3$ with two different concentrations of $ZnSO_4$ (10^{-3} and 10^{-4} M) named a and b respectively. The voltammograms of the two solutions was recorded at room temperature in the potential range from 0.5 to -1.4 V vs. SCE, at potential scan rate of 20mV/s. In the forward scan,two reduction peak were obtained, the first at around -0.7 V vs.SCE [9] related to thiosulfate and the second at around -1 V vs.SCE [10] related to the reduction of zinc ions.No major changes can be easily observed with varying zinc concentration from 10^{-3} to 10^{-4} M. In the return scanning two oxidation peaks were observed related to the oxidation of S and Zn at -0.6 and -0.8 V vs.SCE respectively [11, 12].

The electrochemical deposition process of ZnSis given by the following equations [13-19]:

$$S_2O_3^{2-} + 6H^+ + 4e^- \rightarrow 2S + 3H_2O \quad .(1)$$

$$Zn^{+2} + 2e^- \rightarrow Zn \quad (2)$$

$$Zn + S \rightarrow ZnS \quad (3)$$

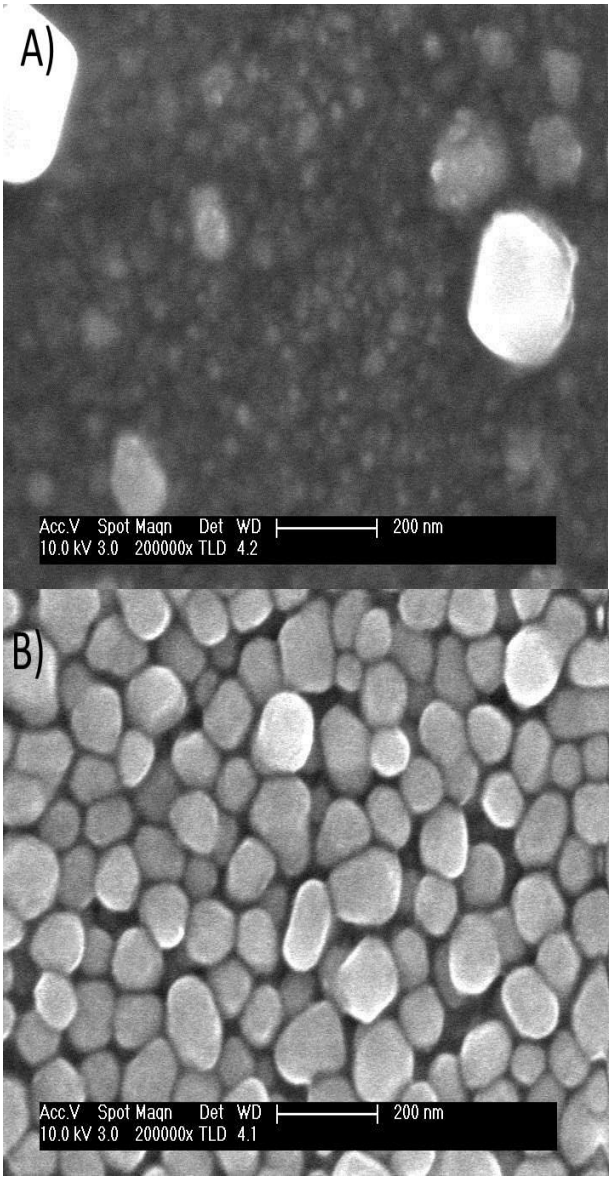

Figure 2. SEM images of the as-deposited ZnS thin films.

3.2 Morphological and structural properties:

The morphology of the deposited ZnS thin films was observed using SEM micrographs. Figure 2 shows the SEM image of the ZnS films electrodeposited from two different $ZnSO_4$concentrations at -1.2V applied potential. A notable change of the form and the size of grain with

decreasing zinc sulphate concentration are observed. For the sample deposited at 10^{-4}M Zinc sulphate (Fig. 02 (b))a granular structure was obtained while the substrate is completely covered with spherical grains uniformly over the whole surface.

Fig. 03 shows the XRD spectra of samples prepared at two different concentration of $ZnSO_4$, the intensity of the peak is found to increase with decreasing zinc sulphate concentration. The intensity of the (200) peak is very strong and it width at half maximum is small, indicating a good crystallization state through a large crystallites size [14]. Hence the apparition of Zinc impurity at 2θ=35.74 and 39.39.correspond to (002) and (100) plan respectively is relative to low concentration of zinc sulfate [20]. While the samples deposited from aqueous solution containing 10^{-3} had no presence of impurity. The crystallite size D was estimated using Scherer's formula given by [21]:

$$D = \frac{0.94\,\lambda}{\beta \cos\theta} \qquad (4)$$

Table. 1: The effect of zinc sulfate concentration on the structural parameters of the electrodeposited ZnS thin films.

	2θ (°)	a (Å)	D (nm)	N_D (cm^{-3})
a	32.91	5.436	63.48	$4.81 * 10^{18}$
b	32.93	5.434	93.55	$7.93 * 10^{21}$

Where, λ is the wavelength of X-ray radiation used, θ is the Bragg angle and β is the full-width at half maximum (FWHM) measured in radian. The average crystallites sizes were given in table 01. The lattice parameter (a) of cubic zinc blend type structure can be calculated using the following formula [22]:

$$a = d_{hkl}\sqrt{h^2 + k^2 + l^2} \qquad (5)$$

Where d_{hkl} is the interplanar spacing corresponding to Miller indices h, k, and l. The calculated lattice parameter (Table 1) is similar to that found in literature [20].

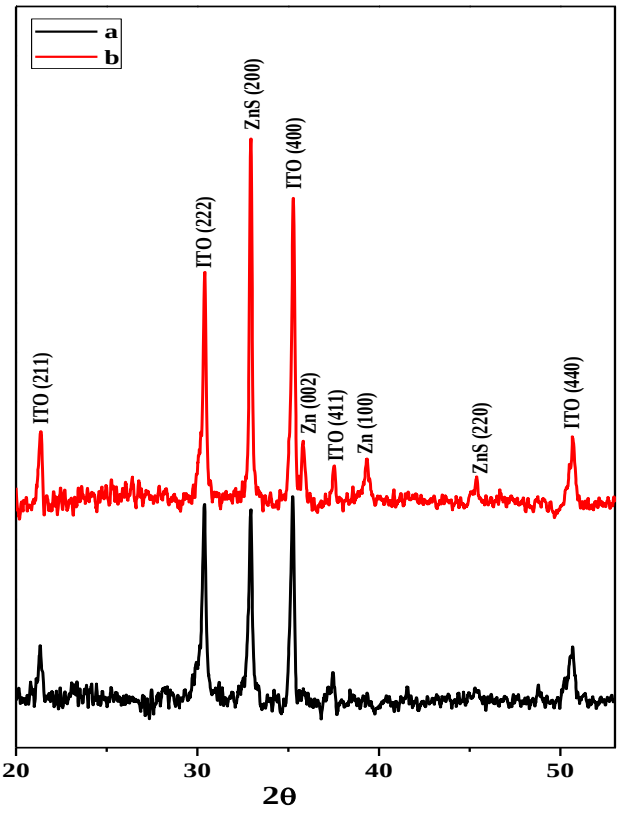

Figure 3. XRD patterns of films deposited at two different concentration of $ZnSO_4$

3.3 Electronic and optical properties:

Electrochemical impedance spectroscopy (EIS) was performed using Mott-Schottky (MS) relation. The capacitance measurements on the electrode/electrolyte interface was also employed to determine the carrier density (N_D), conductivity type and the flat band (E_{fb}), which can be obtained from Mott-Schottky (MS) plot at a fixed frequency of 800 Hz.

The capacitance potential measurements are presented as a Mot Schottky plot following the equation below [21]:

$$\frac{1}{C^2} = \frac{2}{\varepsilon\varepsilon_0 q A^2 N_D}\left(\left(E - E_{fb}\right) - \frac{KT}{q}\right) \qquad (6)$$

In equation (6), C is the interfacial capacitance, ε is the dielectric constant of ZnSε=8.1, ε_0 is the permittivity of free space, k is the Boltzmann constant, N_D is the number density (cm^{-3}) of donor in ZnS, E is the applied potential, E_{fb} is the flat band potential, T is the absolute temperature, and e is the electron charge. The donor density and the flat-band potential of an n-type semiconductor can be obtained from the slope $(= \frac{2}{\varepsilon\varepsilon_0 q A^2 N_D})$ and intercept at C =0[21]. The potential at which the line intersects the potential axis gives the flat band potential (E_{fb}) and the

carrier concentration was calculated from the slope. The positive slope indicate the n type conductivity of the ZnS thin films, from Fig 04 the flat band potential is found to be about-0.268 and -0.12V vs. SCE for the 10^{-3} and 10^{-4} M respectively, this results were similar to that obtained by [22]. When the carrier concentration was about 10^{18} for the first sample, this value are similar to that obtained in literature [23] for the second one, a high number of carrier concentration was obtained (10^{22} cm^{-3}), which may be caused by presence of Zinc found in the X-ray diffraction.

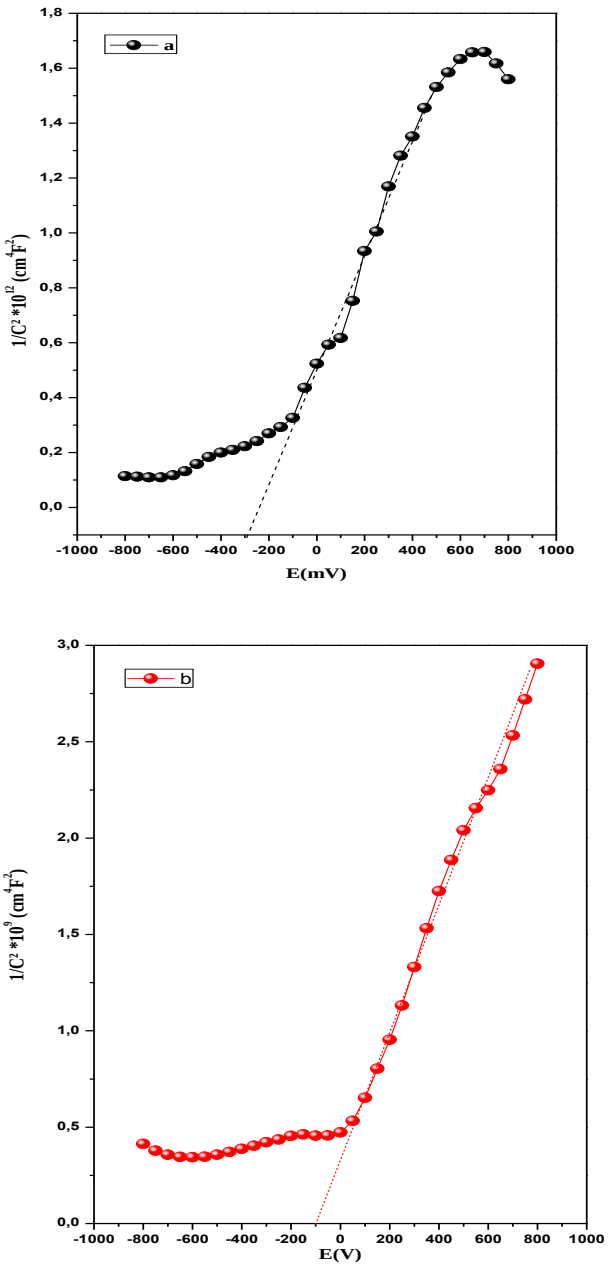

Figure 4. Mott– Schottky plots of the ZnS thin films deposited at a) 10^{-3}M and b) 10^{-4}M of $ZnSO_4$ at 800 Hz.

Transmittance spectrums of ZnS films, with two different concentrations of $ZnSO_4$ recorded in the wavelength range from 250 to 800 nm (not shown here), indicate that ZnS thin films exhibit low trasmittance values, which may be due to the presence of zinc in the films. These values are near to the values for ZnS derived from the electrochemical deposition process [8]. To obtain a high transmittance an annealing process is important for the obtained thin films. The energy band gap (Eg) for ZnS nanostructures was evaluated by using the Tauc plot. The values of the energy band gap of ZnS layers is determined from the intercept of the straight-line portion at the horizontal axis when $(\alpha h\upsilon)^2=0$ (Fig. 5b), the obtained Eg from Tauc plot was 3.37 and 3.88 eV for the films deposited from solution containing 10^{-3} , 10^{-4} M $ZnSO_4$ respectively. This augmentation of Eg is due to the increase in the carrier concentration.

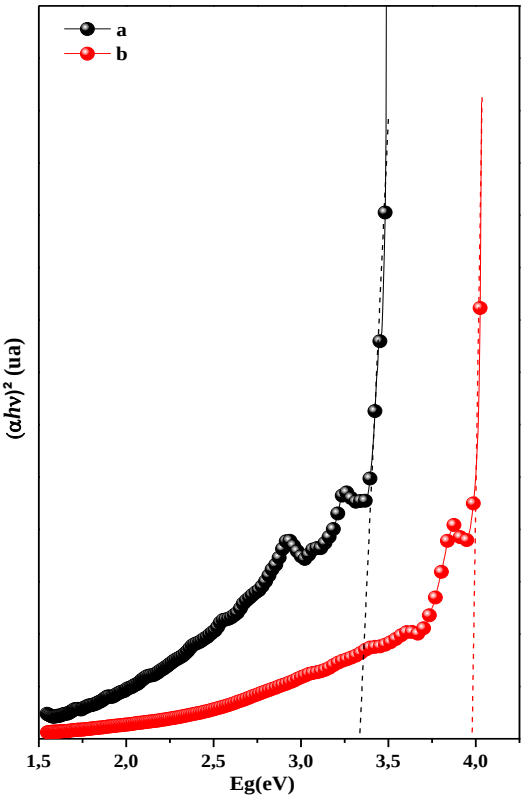

Figure 5. $(\alpha h\upsilon)^2$ vs. energy dependence for the determination of the optical band gap energy of ZnSthin filmson ITO-coated conducting glass surfaces obtained at different $ZnSO_4$ concentrations.

4. Conclusion

In this work we have investigated the effect of $ZnSO_4$ concentration onelectrodeposition process, morphological, structural and optical properties of ZnS thin films electrodeposited on ITO surfaces from sulfate bath. The SEM study shows that varying $ZnSO_4$ concentration has a great influence on the morphological and grain size, XRD show a blend phase structure at room temperature, Mott-Schottky confirm the n type conductivity and the UV-Vis how a high band gap which makes it suitable to use as a widow layer in solar cell application.

References

[1] Dj. Rekioua, E. Matag, Springer, 2012, p 03.

[2] T. Miyawaki, M. Ichimura, Mater. Lett. 61 (2007) 4683–4686.

[3] L. Chabane, N. Zebbar, M. LamriZeggar, M. S. Aida, M.Kechouane, M.Trari, Mater. Sci. Semicond. Process 40 (2015) 840–847.

[4] A. I. Inamdar, Ki-Young Jeon, HyeonSeok Woo, Woong Jung, HyunsikIm. J. Korean Phys. Soc60(2012) 1730-1734.

[5] O.K. Echendu, A.R. Weerasinghe, D.G. Diso, F. Fauzi, I.M. Dharamadasa, J. Electron. Mater 42 (2013)

[6] E. Marquez1, E. R.Shaaban, and A. M. Abousehly, New Horizons in Physics. 1(2014) 17-24.

[7] K. Deepa, K.C. Preetha, K.V. Murali, A.C. Dhanya, A.J. Ragina, T.L. Remadevi, Optik, 125 (2014) 5727–5732.

[8] N. Fathy, M.Ichimura, Energy Materials & Solar Cells, Vol 87 (2005) 747–756.

[9] B. Subramanian, C. Sanjeeeviraga, M. Jayachandran, Mater. Chem. Phys. 71 (2001) 40-46.

[10] G. Riverosa, H. Gomeza, R. Henriqueza, R. Schreblera, R.E. Marottib, E.A. Dalchieleb, Sol. Energy Mater. Sol. Cells 70 (2001) 255-268.

[11] T.Öznülüer, I.Erdoğan, Ü.Demir, Langmuir 22 (2006) 4415-4419.

[12]E.B.Chubenko, A.A. Klyshko, V.P. Bondarenko, M.Balucani, Electrochim.Acta 56 (2011) 4031-4036.

[13] X. Xu, F. Wang, Z. Li, J. Liu, J. Ji, J. Chen, J. ElectrochimicaActa, 87(2013) 511-517.

[14] K. R. Murali, IOSR-JAP,6 (2014), 09-14.

[15] N. Fathy, M. Ichimura, Solar Energy Materials & Solar Cells, 87 (2005) 747–756.

[16] O. K. Echendu, A. R. Weerasinghe, D. G. Diso, F. Fauzi, I.M. Dharmadasa, Journal of electronic materials, 42 (2013) 692-700.

[17] B. Subramanian, C. Sanjeeeviraga, M. Jayachandran, Materials Chem&phy. 71 (2001) 40-46

[18] G.Gomez ,H.Henriquez, R.Sshrebler, R and Cordova,R, SC thin films, 47 (4) (2002), 411-429.

[19] Jung-Yu.L ,Kuo-Chuan.H, Solar energie materials & Solar cels 86 (2005) 229-241.

[20] H.M.M.N. Hennayaka, Ho Seong Lee, Thin Solid Films 548 (2013) 86–90.

[21] M. R. Khelladi, L. Mentar, A. Beniaiche, L. Makhloufi, A. Azizi, J. Mater. Sci. Mater. Electron. 24 (2l013) 153–159.

[22] A. K. Shahi, B. K. Pandey, R. K. Swarnkar, R. Gopal, Appl. Surf. Sci., 257 (2011) 9846– 9851.

[23] Bo Long, Shuying Cheng, Haifang Zhou, Jie Liao, Hong Zhang, Hongjie Jia, Hongnan Li, , ECS Solid State Lett 3 (2014) 140-P143.